PAPER • **OPEN ACCESS**

Numerical analysis of oil injection effects in a single screw expander

To cite this article: S Randi *et al* 2018 *IOP Conf. Ser.: Mater. Sci. Eng.* **425** 012001

View the article online for updates and enhancements.

You may also like

- Research on the Hydrodynamics of the Mechanism of Viscous-Elastic Fluids Displacing Residual Oil Droplets in Micro Pores
Guiling Chen
- Scalably manufactured textured surfaces for controlling wettability in oil-water systems
Manojkumar Lokanathan, Enakshi Wikramanayake and Vaibhav Bahadur
- Application of single-probe fiber optic reflectometry on phase discrimination and velocity and size determination in an oil–gas–water three-phase flow
Jitae Do and Kuang-An Chang

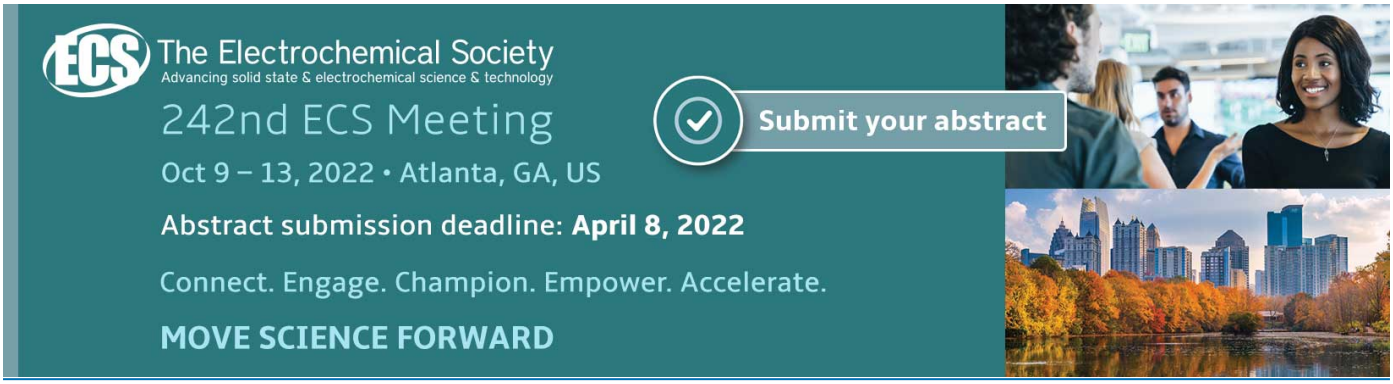

This content was downloaded from IP address 192.167.211.194 on 29/03/2022 at 15:53

IOP Conf. Series: Materials Science and Engineering **425** (2018) 012001 doi:10.1088/1757-899X/425/1/012001

Numerical analysis of oil injection effects in a single screw expander

S Randi[1], A Suman[1], N Casari[1], M Pinelli[1] and D Ziviani[2]

[1]Dipartimento di Ingegneria, Università degli Studi di Ferrara, ITALY
[2]Ray W. Herrick Laboratories, Purdue University, West Lafayette, IN, USA

E-mail: saverio.randi@unife.it

Abstract. The pursuit of higher efficiency for compression and micro-power generation systems has pushed the researchers to an in-depth analysis of positive displacement machines. Single-screw machines, among the others, are gaining attention in the Organic Rankine Cycle (ORC) systems as expanders, thanks to their extended maintenance intervals and compactness. The performances of such devices are strongly affected by the working conditions, and especially the presence of oil has major effects on the operability. The main advantage of adopting an oil-injected device consists in the lube sealing effect, which permits better performance (greater shaft power for assigned boundary conditions) as well as higher reliability. The choice of whether using an oil-free configuration or not is related to the working fluid cleanness, system complexity (oil separator, filters, recovery pump), flow rate and pressure ratio. In this paper, the full 3D numerical simulation of an oil-injected single-screw expander operating with R245fa refrigerant is presented. Oil is injected together with the working fluid at the inlet of the machine. Oily droplets are tracked over the admission duct to show how the oil droplets reach the inlet ports of the screw machine. Different behaviors related to different oil droplet diameters in the range of (0.5 – 50) μm are studied, for the same operating point. The proper distribution of the oil droplets on the screw inlet ports are directly related to the single screw expander performance. In addition, a particular screw position is analyzed for studying the effects of leakages on the oil injection and oil film evolution over the time.

Nomenclature			
C	specific heat [kJ/kg K]	ν	kinematic viscosity [m^2/s]
CFC	chlorofluorocarbon	ODP	ozone depletion potential
CFD	computational fluid dynamics	ORC	organic Rankine cycle
FF	fluid film	σ	surface tension [N/m]
HCFC	hydrochlorofluorocarbon	ρ	density [kg/m^3]

1. Introduction

The increasing energy demand, together with the need of a cleaner way of production, has raised the attention of industry and researches towards the recovery of energy from low-quality heat sources.

Content from this work may be used under the terms of the Creative Commons Attribution 3.0 licence. Any further distribution of this work must maintain attribution to the author(s) and the title of the work, journal citation and DOI.
Published under licence by IOP Publishing Ltd

Among the others, the use of Organic Rankine Cycles (ORCs) is constantly growing, ranking this technology as the most employed one for generating power from low-grade heat [1]. Evidence of the increasing interest into this topic is the number of research papers: whereas almost 100 research papers were published from 2005 to 2014, in the sole 2015 the same number of publications has been reached [2]. Within the low-grade heat recovery framework, a great part of the applications regards source power that are lower than 100 kWe. To this range, the class of so called micro and mini ORCs applies. This work deals with this class of power plants. The research about this topic regards mainly the improvement of the overall efficiency.

Mini and micro-ORCs overall efficiency is strongly affected by the efficiency of two of their components: the expander and the feeding pump. In light of this remark, it is obvious that such components have been thoroughly studied. For small scale cycles, usually volumetric pump and expanders are used, and this last machine is the component that is receiving attention the most, see for example [3-5]. Due to the smaller volume flows inside these systems, non-conventional expansion technologies such as screw expanders become more interesting. Particularly, due to their cost effectiveness, screw machine has been widely employed for this kind of application [4,6], mostly deriving the expander from compressors used the other way around [7].

Screw-type machine are divided in two main families: twin and single screw devices. The vast majority of the applications see the employment of the first one. The use of single screw devices is still marginal, even if they have some pros with respect to the twin-ones: for example, the force-balanced operation thanks to their mechanical layout [8] is a highly appreciated feature of this machine. Contrarily, a weakness of the single screw configuration is related to the relatively high flow leakages between regions of the machine at different pressures. One way to overcome such an issue is to inject a certain amount of oil within the working fluid. The oil acts as a sealant agent between the various parts of the device, closing leakages paths, lubricating and, moreover, cooling the machine. It is then necessary to study how device working conditions are affected by the presence of such a "sealant", in terms of efficiency thickness of the oil film and zones in which fluid can stagnate or affect the normal behaviour of the expander.

Several studies regarding the development of dynamic models of oil injected and oil flooded ORCs are reported in literature, like [4] and [5], mainly with the objective of increasing the thermodynamic efficiency of the system. Stosic et al. [9] developed a model to account for the injection of oil during the working cycle of a twin-screw compressor, finding that oil injection ports position strongly affects power and volumetric efficiencies. Stosic et al. [10] ran several multivariable optimizations to design twin-screw compressors capable of obtaining better efficiencies than the ones designed using classical approaches: in their calculations, they calculated optimum conditions for oil flow and temperature, together with the angular position of the injector inside the casing, for a machine working with air and another using R134a. De Paepe et al. [11] showed that the atomization of oil inside a screw compressor permitted to cool down the device, but did not strongly affect its global performance, thus excluding this approach to obtain an isothermal compression. Ziviani et al. [12], when studying a micro-ORC whose expander has been adapted from a single-screw compressor, observed that by halving leakages and friction losses, isentropic efficiency could reach values of above 70 %: to reduce friction and leakages, one way is to increase the amount of oil circulating in the expander.

To the writer knowledge, very few works have been done to analyze oil thickness on the different parts of the machine, and no one involved the analysis of a screw machine. For example, Minami et al. [13] compared oil film thickness for a rolling piston compressor when using R410a in place of R22 refrigerant, while Hotta et al. [14] evaluated lubricant distribution inside a swash plate compressor by means of an experimental campaign, differently from the approach of Minami et al. [13], that was numerical. In both cases, they concluded that for a reliable operation during the whole machine life cycle, the oil film on the meshing parts has to remain constant and it must not break. The advantages of having a constant film height on the moving parts consists in the possibility of removing low friction materials from the contacting components, thus saving money and weight.

Looking at ORC applications, depending on the refrigerant used in the cycle, several types of oil are

available. Provided that CFC and HCFC refrigerants are no more employed due to their non-zero Ozone Depletion Potential (ODP), ester-based oils are used when dealing with HFC refrigerants [15]. Since oil influences properties of the working fluid in which it mixes, different works has been done to investigate properties of such mixtures, such as the ones by Zhelezny et al. [16] or Marsh and Kandil [17]. For example, Zhelezny et al. [16] studied concentration dependencies for vapor pressure, density, surface tension and capillary constant for a R245fa-polyolester compressor oil mixture. The usefulness of this work is due to the fact that different oil concentration in refrigerant are used in the works reported in literature, e.g. Ziviani et al. [18] studied the behavior of a single-screw expander using, as working fluid, a mixture where lubricant concentration was 3 % vol., while Hiwata et al. [19] analyzed how the performance of a CO_2-scroll compressor are affected by the injection of up to 25 % wt. of oil in the working fluid.

In light of these considerations, in this work a 3D transient CFD simulation of an oil-injected single screw expander has been carried out. Experimental characterization of such machine has already been done by Ziviani et al. [12], thus data for mass flow rate, temperature and pressure values of the working fluid at the inlet and outlet sections of the device are known. Furthermore, the same expander has already been modelled by means of CFD techniques, when operating without lubricant oil [20]: both in that work and the present one, Simcenter STAR-CCM+® has been the software used to carry on the simulations. The present work reports two different analyses. The first analysis is related to the droplet and oil film evolution inside the inlet distributor (that is characterized by a particular shape due to position of the ports) according to different droplet size for the same gas and oil mass flow rate. The second analysis is related to a particular geometric condition for which the position and the shape of the screw determine the complete closure of both inlet ports. In this condition, the instantaneous mass flow rate operated by the expander is only due to leakages between screw, case and star wheels, and for this reason, the oil droplets are affected by different behavior compared to those highlighted in the first analysis.

2. Single-screw expander geometry and CFD model

The machine considered in this work is an 11 kWe air compressor which is used as an expander for micro organic Rankine cycle (ORC) systems. Ziviani et al. [21] have already depicted in detail the dimensions of the device; however, for the purposes of this approach, the real geometry (Figure 1a) has been simplified in several details. All the bearings and main rotor and starwheels shafts, have been simplified, as well as the sealings; on the other hand, the external housing has not been changed, in order to predict flow behavior from the main inlet port of the machine to the screw, throughout the admission duct characterized by a curved shape. In addition, all the clearances have been modelled. According to Ziviani et al. [20], the clearances between the screw and case are in the range of (0.03 – 0.06) mm, while the clearances between the starwheel and the screw are in the range of (0.02 – 0.06) mm.

Since, within the considered simulations, oil is introduced at the main inlet of the machine, the two injectors already present in the geometry have not been used. Instead, a cone injector has been modelled and placed coaxially to the main inlet (represented by the violet circle in Figure 1b), in order to uniformly spread lubricant particles in the bulk flow of gas. Following the gas path, the mixture (refrigerant gas and oil droplet) is then injected in the expansion chamber of the screw rotor by means of two admission ports, represented in Figure 2. As can be seen from Fig. 2, the two admission ports are not symmetric with respect to the screw rotor and for this reason, the oil droplet behavior and the oil film evolution over the entire admission duct will be different according to the side. According to the geometry, the upper port is closer to the main inlet section while, the gas path of the lower port is characterized by two narrow bends.

2.1. Numerical models

To simulate the behavior of this kind of machine, different models have been used in STAR-CCM+®. While the capability of this software to deal with single-screw expander moving parts has already been proven (Ziviani et al. [20]) this time, while no rotating parts have been modelled by means of overset

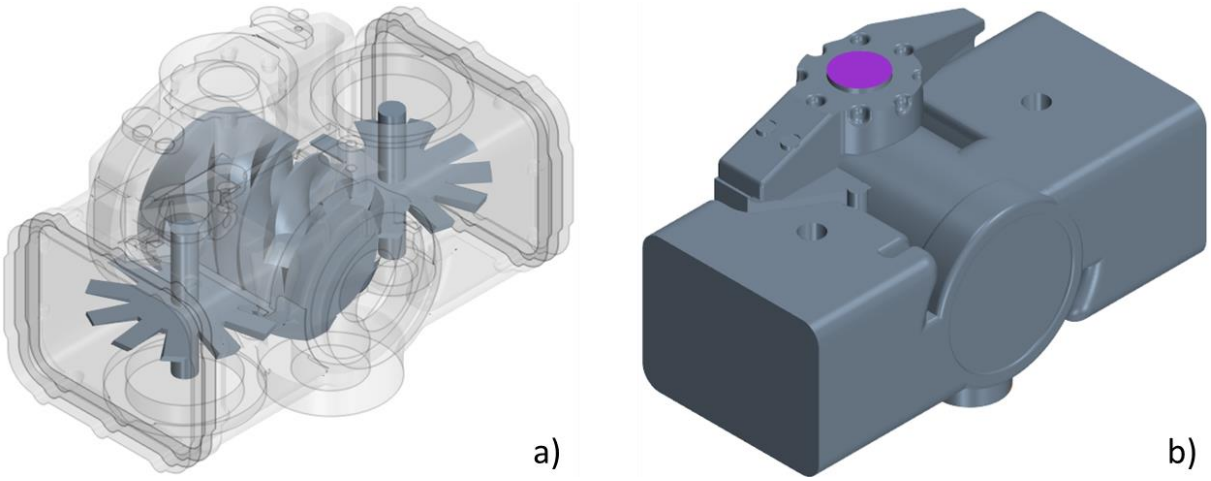

Figure 1. Single screw expander: a) CAD model (external case, screw rotor and two starwheels) and b) fluid model (the main inlet port is highlighted in violet).

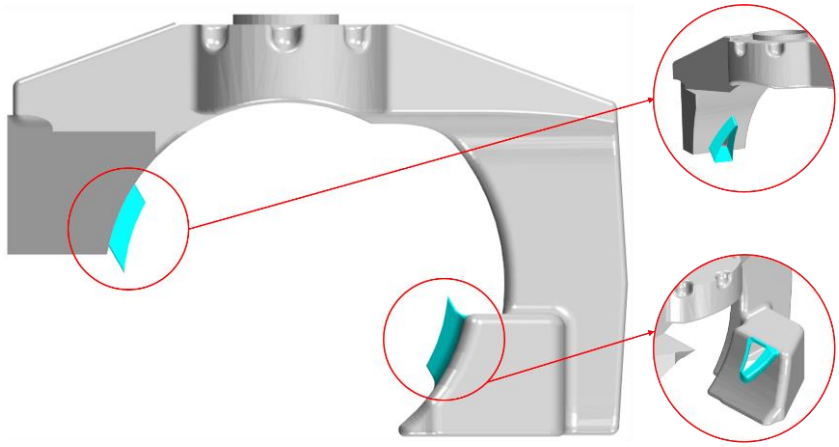

Figure 2. Front view of the inlet duct with the upper and lower admission ports (cyan).

meshes (screw rotor and starwheels are considered fixed), the presence of dispersed liquid lubricant droplets inside the bulk flow represented another challenge. To deal with this peculiarity, the working fluid has been modelled as real gas with Redlich-Kwong equation of state (EoS). The Eulerian approach has been coupled with Lagrangian one, to track oil droplets from the injection point to machine surfaces: since these droplets were predicted to form a film in the expander parts, also the fluid film and impingement models were enabled, together with the edge stripping one to take into account oil stripping from the different parts of the machine. In this paragraph, a short description of each of these models will be presented.

Redlich-Kwong EoS is one of the several equations which have been proposed in the last decades to consider the behavior of gases in those regions of the p-v-T diagram characterized by temperatures near the critical one and pressures far from the critical value. In particular, this one models gas by modifying the ideal gas law with the introduction of two coefficients *a* and *b*, which are both functions of the gas temperature and pressure at its critical point. It has to be noticed that physical conditions of R245fa in our case are very close to the ideal gas behavior at the outlet of the machine (Z=1.01), while at the inlet a compressibility factor near 0.83 indicates that an ideal gas approach would not be appropriate. The gas bulk flow receives oil droplets which are modelled with a lagrangian approach, which is the most suited in case of dispersed droplets in a continuous phase. This approach allows the tracking of each single droplets, highlighting the single behavior in terms of velocity, dimension, temperature, etc. Since solving a set of equations for each droplet would be excessively time consuming, the CFD software

adopts a statistical approach in which all the droplets are grouped in clusters, which are representative group of droplets which share the same properties. For the sake of the analysis presented in this work, the so-called "two-way coupling" model has been enabled, in order to take into account the exchange of momentum and energy of the droplets with the working fluid, not only the vice versa. Furthermore, since it is expected that these droplets collide with expander surfaces, an impingement model had to be used. In the case of a wet boundary, the liquid particle transfers its mass, momentum and kinetic energy to the fluid film, making it necessary to evaluate the latter's properties by means of the fluid-film (FF) model. Moreover, this is necessary because it is expected that, when reaches a sharp edge, liquid will drip on the underlying surfaces.

The fluid film model solves equations for mass, momentum and energy conservation, together with the computation of the volume of liquid film in each of the cells of the numerical grid. The results are FF pressure, temperature, distribution and thickness. In our case, FF accumulates due to the impinging particles, while its thickness is reduced due to film stripping. This latter phenomenon is modelled thanks to the approaches proposed by Friedrich et al. [22] when considering the liquid film break-up criterion, and the one suggested by Maroteaux et al. [23] for calculating the diameter of droplets which result from stripping. Fluid will separate from an edge when the ratio of inertial force to the surface tension and gravitational force is greater than one; this ratio also affects the number of droplets which are ejected from the bulk flow, where their velocity is the same as the film one. All the simulations performed in the present work are realized by considering the conjugate heat transfer between gas, oil droplets and oil film. The walls are considered adiabatic.

In Table 1, the values of the materials properties and boundary conditions defined in the current work are reported. The transient simulation was performed by imposing a time-step of 5e-7 s that corresponds to a maximum Courant number of 1. To model turbulence, the two-equations, shear-stress transport (SST) k-ω model of Menter [24] has been adopted. Oil is introduced in the numerical domain with an injector modelled as a solid cone, which means that lubricant was injected in the form of uniformly distributed parcels from the base of the cone in seven random directions. This configuration has been considered because premixing oil and refrigerant upstream the expansion chamber is the simplest way of retrofitting a pre-existing machine with a lubrication system, since the alternative is to place an injector near the meshing zone of each starwheel with the screw. The temperature of oil has been chosen to be lower than the refrigerant one in order to take into account the possible lowering of machine components temperature due to the impinging fluid. To initialize lubricant film calculations, a height of 1 μm has been imposed on all the boundaries which were expected to be covered with oil, namely the inlet ducts, the starwheels and the screw. The minimum sharp edge angle at which oil is permitted to strip has been set to 10 degrees. The lubricant properties were defined as functions of temperature, using data presented by Zhelezny et al. [16] and reported in the oil datasheet. Relations for the temperature-varying properties are listed below.

$$\nu = 1.5748\text{e}39\ T\exp(-17.258)$$

$$\rho = 3.5987\text{e}3\ T\exp(-0.23055)$$

$$\sigma = 2.2684\ T\exp(-0.77639)$$

$$C = 6.7533e\text{-}2\ T\exp(0.57540)$$

Table 1. Model properties and boundary conditions.

Properties	Value	Properties	Value
R245fa Inlet Temperature [K]	398.05	Oil Droplets Diameter [μm]	0.5 – 50
R245fa Dynamic Viscosity [Pa s]	1.3723e-5	Oil Inlet Velocity [m/s]	4
R245fa Specific Heat [J/kg K]	1102.3	Injector Cone Angle [rad]	2
R245fa Thermal Conductivity [W/m K]	0.021519	Injector Streams [-]	7
Oil Inlet Temperature [K]	340	Engaging Ratio [-]	11/6

2.2. Mesh

Two numerical domains have been meshed according to the analysis type. As mentioned, the first analysis is devoted to the comprehension of the oil droplet and film behavior inside the inlet distributor. The numerical domain (reported in Fig. 2) was discretized by means of half million hexahedral elements with dimensions spanning from 0.5 to 2.0 mm. The numerical grid realized for the inlet distributor is reported in Fig. 3a. In relation to the second analysis, the numerical domain (reported in Fig. 1b) was discretized by means of hexahedral elements, with dimensions spanning from 0.01 mm to 2.0 mm, as reported in a previous work [20] in order to account for the gaps between screw rotor, case and starwheels. This led to the generation of a near two-million-elements mesh, which has guaranteed a good compromise between computational and solution accuracy. The present meshes are chosen after a grid sensitivity analysis. In Figs. 3a-b, both a section of the domain, and a representation of the numerical grid on the moving parts of the machine are shown.

The combination between elements dimensions and flow characteristics led to y^+ values in the range 0.5-100; this fact suggested to choose an all-y^+ approach, leading to the solution of the viscous sub-layer for those value of y^+ <1 and the use of wall functions for values outside the transition zone.

3. Results

3.1. Inlet distributor analysis

This analysis was carried out in order to highlight the different behaviors which affect the oil droplets characterized by different diameter. In particular, three diameters have been considered in the range of (0.5 – 50) μm. This range is selected according to the literature values [25, 26], and in addition, this wide droplet size range is useful for performing a detailed sensitivity analysis. In the present analysis, the mass flow rate at the main inlet is imposed equal to 0.3 kg/s according to the experimental results reported by Ziviani et al. [12], while, an outlet static pressure equal to 1.3 MPa is imposed on both inlet

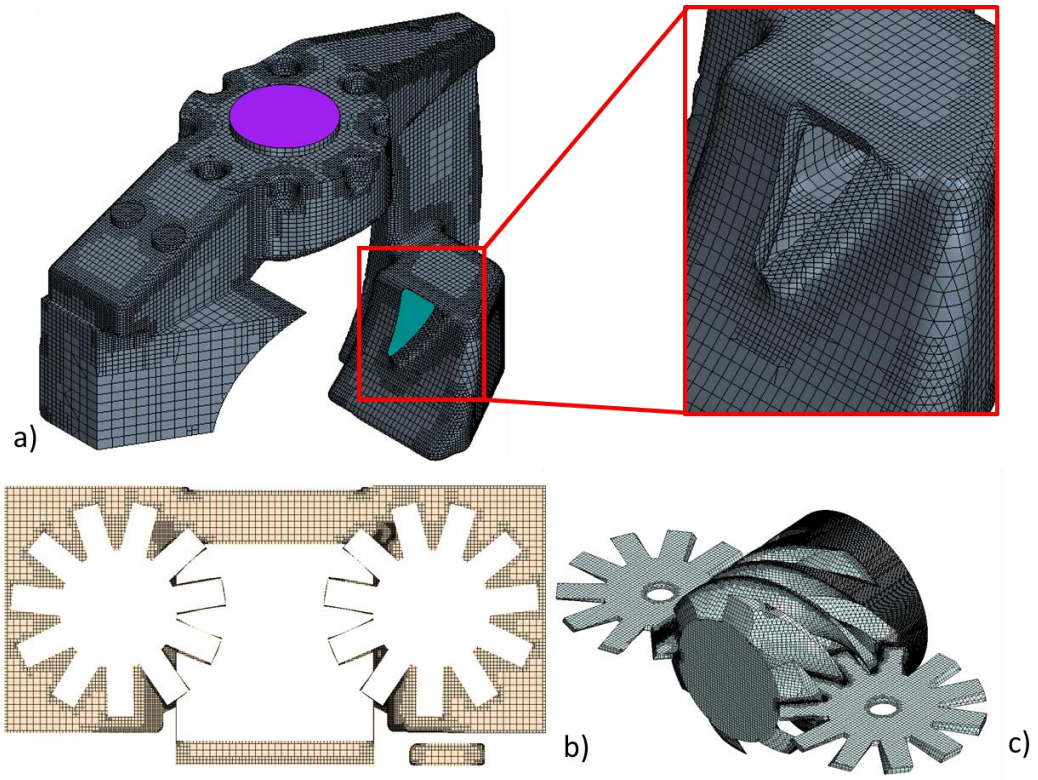

Figure 3. Numerical grids: a) on distributor duct, b) section plane perpendicular to wheels axes and c) on rotating parts.

ports. At the same time, the oil mass flow rate was imposed equal to 0.003 kg/s that corresponds to the 10 % in weight. This weight rate is imposed according to the analysis reported in [4]. The oil droplets were injected after the resolution of the flow field in order to realize a transient analysis of the oil film evolution over the time.

According to these conditions, Table 2 reports the results obtained for the three analyses according to the three particle diameters. As shown in the table, the number of droplets at the inlet ports of the screw changes according to the droplet diameter. The particular shape of the inlet distributor determines several differences of flow field over the flow path. Considering the streamlines reported in Figure 4, it is possible to see that the lower inlet port is affected by eddy structures due to the bent shape of the duct, while the upper port is located immediately downstream of the of the high-radius 90° curve (see Fig. 2 for completeness). The deviation upstream the lower port, influences the droplets trajectories and, for bigger particles, the droplet inertia determines huge deviations from the gas streamlines, as reported in Figure 5. For this reason, the biggest droplets are not able to reach the lower port. In the case of smaller droplets, the trajectories (see Fig. 5a-b) appears more similar to the gas streamlines (see Fig. 4) and in turn, the oil droplets are able to reach the upper and lower port.

In an actual application, the oil injector is responsible of a certain droplet diameter distribution (see for example [25] and [26]) and, in the light of the present results, the proper analysis of the droplet distribution, the location of the injector and the inlet distributor shape is needed. In a general way, and in the presence of a general droplet diameter distribution, smaller droplets are able to follow the gas streamlines, but they are responsible only for a minimum part of the oil mass flow rate. This fact could generate several issues related to the friction losses and wear in a specific region of the machine.

At the inlet ports of the screw, not only the oil droplets are responsible of the lubricant action of the

Table 2. Oil droplet analysis for the inlet distributor.

Oil droplet diameter [μm]	**Oil droplets @ upper port [%]**	**Oil droplets @ lower port [%]**
0.5	0.99	0.03
5.0	3.39	0.05
50	5.69	0.00

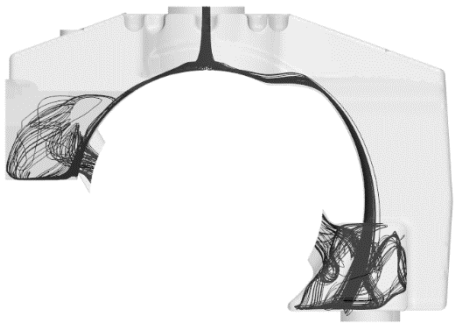

Figure 4. Gas streamline in the inlet distributor.

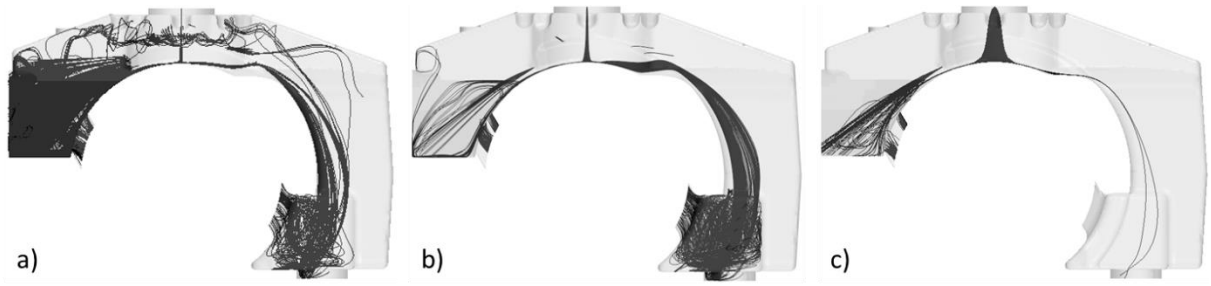

Figure 5. Oil droplet trajectories: a) 0.5 μm b) 5.0 μm and c) 50.0 μm.

oil on the screw walls but also the oil film. This is generated in the inlet distributor by the oil droplets, and moves towards the ports, thanks to the gravity action and to the drag action provided by the gas. Considering the snapshots reported in Figure 5, the trajectories of the oil droplets released by the injector at the main inlet are clearly visible. In Figure 6, the oil film distribution in the inlet distributor are reported. The oil film is representative of 0.4 s of oil injection. It is clearly visible how the oil film grows in the front of the injector and moves down, according to the distributor walls. At the screw inlet ports, the oil film strips and it is dragged towards the screw. In the next section, an analysis related to the interaction between oil film and the rotor screw will be reported in detail.

3.2. Screw rotor interaction analysis

This second analysis is carried out in order to highlight a particular geometric condition for which the position and the shape of the screw determine the complete closure of both inlet ports. As mentioned, in this configuration, the instantaneous mass flow rate that flows over the single screw expander is only due to leakages between screw, case and star wheels. Therefore, the oil droplets are affected by different behavior compared to those highlighted in the first analysis. In the present analysis, the static inlet pressure equal to 1.3 MPa is imposed at the main inlet, while a static pressure equal to 0.3 MPa is imposed at the single screw outlet in agreement with Ziviani et al. [12]. In addition, the rotational velocity is applied to the screw and starwheel walls equal to 3000 rpm and 1636 rpm respectively. In the same way of the first analysis, the oil droplets were injected after the resolution of the flow field in order to realize a transient analysis of the oil film evolution over the time. The relative position of the screw rotor and the upper port is reported in Figure 7 (the upper port trace is depicted in red). In this

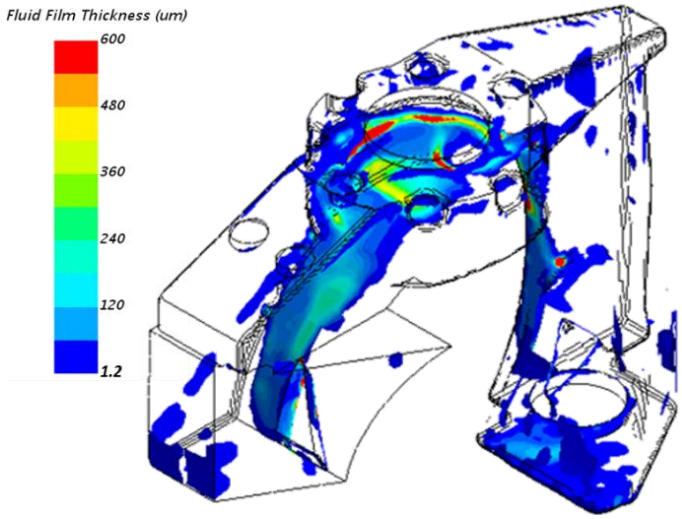

Figure 6. Oil film on the inlet distributor walls (0.4 s).

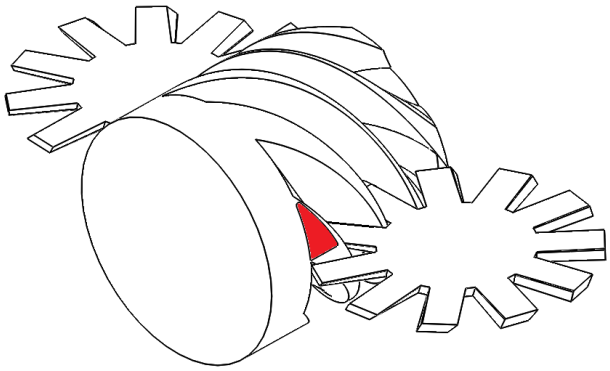

Figure 7. Relative position between inlet port (in red) and screw: the screw thread totally occludes the inlet port.

configuration, the inlet port is affected by a not negligible stagnation and the consequent back pressure. In the following, the oil film thickness variation over the time, pressure and velocity fields are proposed with the aim of highlight the fluid dynamic phenomena given by the contemporary presence of real gas expansion and fluid film behavior.

The results reported here refer to a transient analysis of 0.4 physical seconds. This limited period was sufficient to obtain information about oil distribution and its effect on the flow field on the inlet distributor and on the screw rotor walls. In Figure 8, the oil film thickness on the screw walls, obtained with oil droplet of 50.0 μm, is reported. In addition, the position of the upper port is highlighted in pink. As can be seen from Figure 8, on the lower part of the screw walls the oil film is thicker and involves the screw groves in the proximity of the starwheels surfaces, even if, the maximum thickness seems to be located downstream the engagement zone. This fact is due to the oil droplet trajectories. As reported in Figure 9, the oil droplets escape towards the lower part of screw rotor according to the pressure gradient. As can be seen in Figure 10, the inlet pressure characterizes only the screw region immediately downstream of the upper port (the red region with the triangular shape), while lower pressure values (the discharge pressure of the single screw expander) characterizes the other screw regions.

Taking into consideration the oil film distribution, reported in Figure 8, and the pressure field reported in Figure 10, another important consideration can be done. Part of the oil droplets is dragged towards the rear part of the screw due to the difference of pressure between the incoming working fluid and the lower pressure existing in that part of the domain. Looking at Figure 8, which depicts oil thickness, it is apparent that the two phenomena are related. In that zone, the height of the lubricant film is comparable with respect to the entire domain. As depicted in Figure 10, the inner screw region (in the

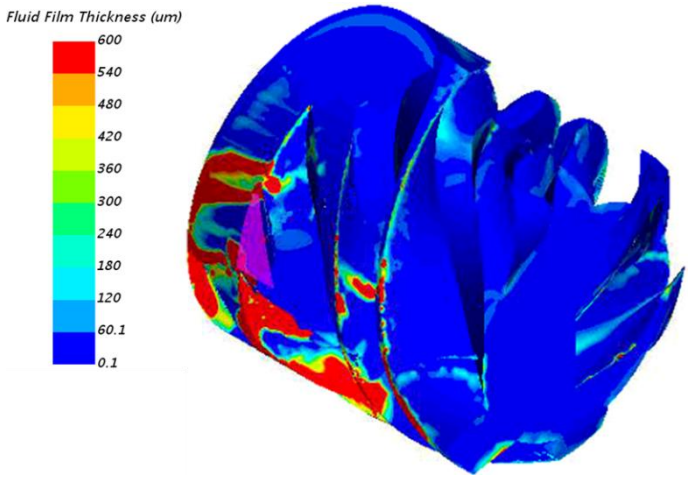

Figure 8. Oil film thickness on the screw walls (the upper port is highlighted in pink).

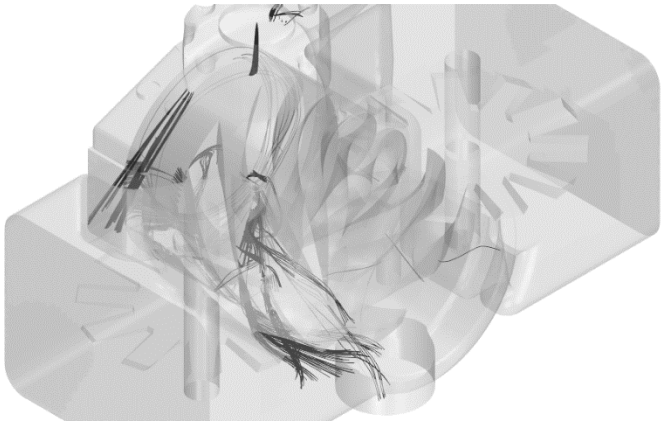

Figure 9. Oil droplet trajectories on the single screw expander.

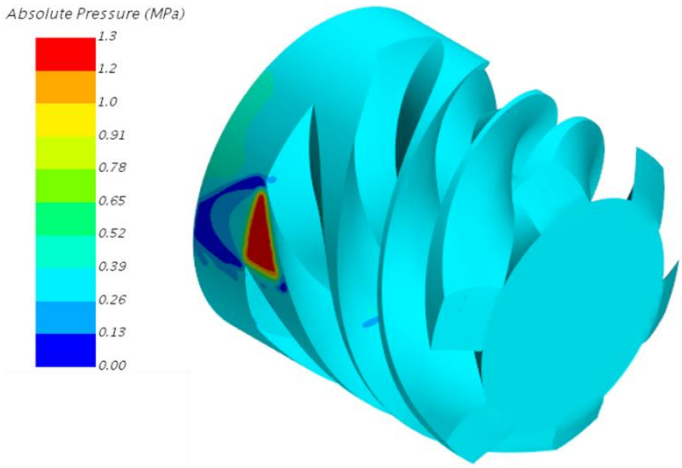

Figure 10. Pressure field on the single screw expander.

proximity of the inlet port) is characterized by huge pressure gradient (equal to about 1.3 MPa) generated by the effect of the gaps between screw and casing and the stagnation provided by the screw thread. This is confirmed by looking at Figure 11, in which the gas streamline colored by velocity are tracked over the single screw expander. Looking at the upper port, the leakage flow of refrigerant is particularly strong immediately downstream the admission port, giving an opposite direction with respect to the usual one. When the mixture oil-refrigerant exits the admission port, it is split in two directions, upstream and downstream the position of the port.

For the present machine setup, in this localized region, the gap between the casing and the screw determines a not negligible leakage. The combination of this radial gap and the pressure field (see Figure 10) determines a relevant oil stagnation. On the other hand, this stagnation causes a reduction of nearly 60 % of the gap between the screw and the casing (calculated considering the height of the oil film with respect to the total clearance of roughly 1 mm), thus reducing leakages in the rear part of the machine. Unfortunately, by injecting the oil at the inlet port, this beneficial effect is not obtained in other zones of the screw, or in the meshing area between this component and the starwheels, since oil drips from the inlet duct and it is scavenged only in one direction. This effect is accented by the distribution of the lubricant on the inlet distributor (see for example Figure 6).

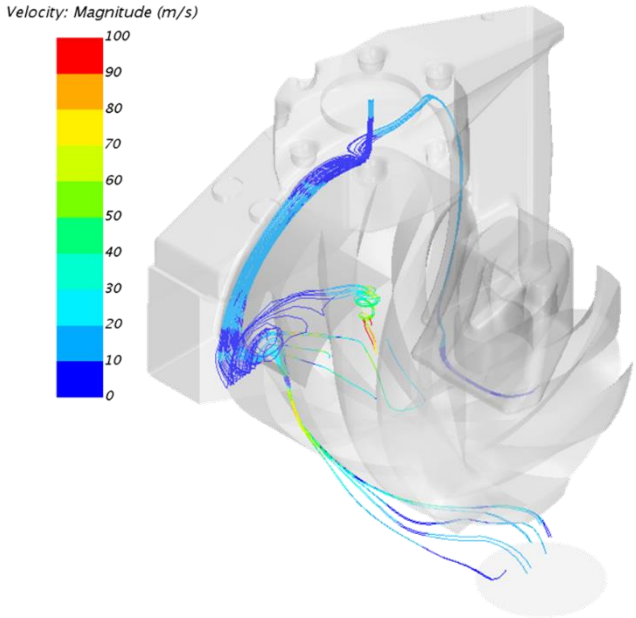

Figure 11. Gas streamline over the single screw expander colored by velocity.

By means of transient simulation, it is possible to discover the oil film progression over the time. Figure 12 depicts different frames, according to the physical time reported for each instant, of the oil film thickness, starting from the initial formation in front of the injector, to the final stripping on the screw rotor walls. At the beginning, the oil film assumes a circular shape according to the injector shape (cone injector) and it appears not equally distributed with respect to screw mid-plane. This result is probably due to the effect of the leakages that affects this particular geometric condition of the single screw expander.

Soon after, the oil film flows towards the upper port (see Figure 2) whose feeding duct is characterized by higher slope than the other one. Therefore, the action of gravity force is predominant over the drag force provided by the incoming gas. For the same reason, the oil droplets are not able of being distributed over the entire duct surfaces and they accumulate mostly in the lower surfaces. When the oil film reaches the admission port, it is split in two ways: one in the lower part of the screw rotor and the other one downstream the inlet port.

Taking into consideration the oil film thickness (see Figures 8 and 12), in the presence of narrow passages, and/or in the presence of high gas velocity, the reduction of the passage area due to the oil film, could generate a sort of blockage with consequent increment of pressure losses. This means that the position of the injector, the oil flow rate and the machine configuration play a double role: on one hand, an increase in the machine efficiency by reducing the friction losses and flow leakages can be expected, but on the other they can have a detrimental effect on machine performance by reducing the flow passage area and causing windage losses.

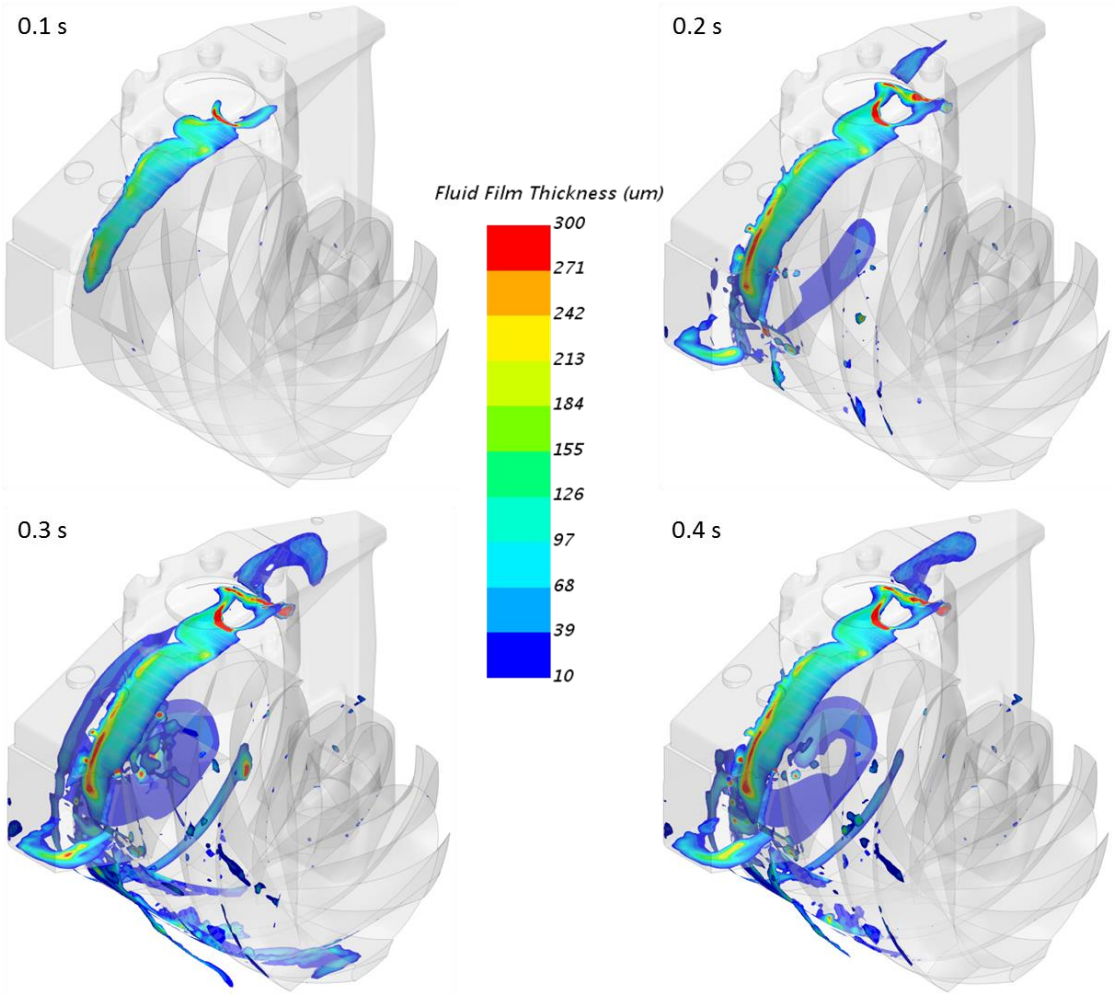

Figure 12. Oil film thickness time evolution from the inlet to the screw rotor.

4. Conclusions

In the present paper, the numerical simulation to study the effects of oil injection on the operating conditions of an actual single-screw expander has been carried out. The lubricant injector has been placed at the inlet port of the machine, with the oil driven by the R245fa to the expansion chamber.
A two-step analysis has been carried out. Firstly, the oil droplets trajectories in the inlet distributor are investigated, as well as the oil film that grows on the wall as oil keeps on impinging. Secondly, the same analysis is carried out on the entire machine, freezing the rotors in the instant where both the inlet ports are completely *shut*. In the first analysis, the effect of three different sizes of droplets has been considered (0.5 μm, 5.0 μm, and 50.0 μm), while for the entire machine, only the 50.0 μm droplets have been simulated.

From the first analysis, it is clear how the particle size affects the overall presence of oil inside the screw machine. Particularly, the high inertia of bigger particles tends to make them impinge on the inner walls of the distributor. Only a small amount of the droplets is able to make its way to the inlet upper port without being entrained in the thin fluid film that flows over the walls.
In light of this is mainly the fluid film that enters the working chamber, being stripped immediately downstream the inlet port. Such film is mainly transported towards the rear part of the screw, making the lubrication of the screw ineffective in the configuration under analysis.

From this work, it is clear that the smallest droplets have the higher probability to reach the actual working chamber, without impinging on the walls. Therefore, an efficient lubrication is obtained by decreasing droplets diameter (choosing an oil with lower viscosity and surface tension or by mounting a nozzle with a different geometry) or adopting a different configuration for the injectors (e.g. by placing them in a position where lubricant drops on the meshing pair, without being dragged by refrigerant flow). The simulation of a fully transient, dynamic mesh simulation is to be considered the next step of this analysis, showing the path the fluid film follows when the dynamic of the machine is considered.

References

[1] Quoilin S and Lemort V 2009 *Proc. 5th European Conference Economics and Management of Energy in Industry* (*Vilamoura*) pp. 459–64.
[2] Landelle A, Tauveron N, Haberschill P, Revellin R and Colasson S 2017 *Appl. Energy* **204** 1172-87
[3] Bao J and Li Z 2013 Renewable and Sustainable Energy Reviews **24** 325-42
[4] Ziviani D, Gusev S, Lecompte S, Groll E A, Braun J E, Horton W T, van den Broek M and De Paepe M 2016 *Appl. Energy* **181** 155-70
[5] Ziviani D, Gusev S, Schuessler S, Achaichia A, Braun J E, Groll E A, De Paepe M and van der Broek M 2017 *Energy Procedia* **129** 379-86
[6] Tang H, Wu H, Wang X and Xing Z 2015 *Energy* **90** 631-42
[7] Papes I, Degroote J and Vierendeels J 2013 *Int. Mechanical Engineering Congress and Exposition* November, 15-21 2013 San Diego
[8] Zimmern B and Patel G C 1972 *Int. Compressor Engineering Conference* West Lafayette
[9] Stosic N, Kovacevic A, Hanjalic K and Milutinovic Lj 1988 *Int. Compressor Engineering Conference* West Lafayette
[10] Stosic N, Smith I K and Kovacevic A 2003 *Appl. Thermal Eng.* **23** 1177-95
[11] De Paepe M, Bogaert W and Mertens D 2005 *Appl. Thermal Eng.* **25** 2764-79
[12] Ziviani D, Gusev D, Lecompte S, Groll E A, Braun J E, Horton W T, van den Broek M and De Paepe M 2017 *Appl. Energy* **189** 416-32
[13] Minami K, Hattori H and Hayano M 1998 *Int. Compressor Engineering Conference* West Lafayette
[14] Hotta T, Inoue T, Matsuda M and Ueda M 2004 *Int. Compressor Engineering Conference* West Lafayette
[15] Whitman B, Tomczyk J, Johnson B and Silberstein E 2013 *Refrigeration & Air Conditioning Technology* (New York: Delmar Cengage Learning)

[16] Zhelezny V P, Semenyuk Yu V, Ancherbak S N, Grebenkov A J and Beliayeva O V 2007 *Journal of Fluorine Chemistry* **128** 1029–38
[17] Marsh K N and Kandil M E 2002 *Fluid Phase Equilibria* **199** 319-34
[18] Ziviani D, Desideri A, Lemort V, De Paepe M and van den Broek M 2015 *IOP Conf. Ser.: Mater. Sci. Eng.* **90** 012061
[19] Hiwata A, Iida N, Futagami Y, Sawai K and Ishii N 2002 *Int. Compressor Engineering Conference* West Lafayette
[20] Ziviani D, Suman A, Gabrielloni J, Pinelli M and De Paepe M 2016 *Int. Compressor Engineering Conference* West Lafayette
[21] Ziviani D, Bell I, De Paepe M and van den Broek M 2016 *Int. Compressor Engineering Conference* West Lafayette Paper n.1486, pp. 1-10.
[22] Friedrich M A, Lan H, Drallmeier J A and Armaly B F 2008 *J. Fluids Eng* **130** (5)
[23] Maroteaux F, Llory D, Le Coz J-F and Habchi C 2002 *J. Fluids Eng.* **124** 565-75
[24] Menter F R 1994 *AIAA Journal* **32** 1598-605
[25] Stosic N, Milutinovic Lj, Hanjalic K and Kovacevic A 1992 *Int. J. Refrig.* **15** 206-20
[26] De Paepe M, Bogaert W, Mertens D 2005 *Appl. Therm. Eng.* **25** 2764-779

Acknowledgments
The research was partially supported by the Italian Ministry of Economic Development within the framework of the Program Agreement MSE-CNR “Micro co/tri generazione di Bioenergia Efficiente e Stabile (Mi-Best)”.